AIP | Review of Scientific Instruments

Polarization-modulation near-field optical microscope for quantitative local dichroism mapping

L. Ramoino, M. Labardi, N. Maghelli, L. Pardi, M. Allegrini, and S. Patanè

Citation: Review of Scientific Instruments **73**, 2051 (2002); doi: 10.1063/1.1470710
View online: http://dx.doi.org/10.1063/1.1470710
View Table of Contents: http://scitation.aip.org/content/aip/journal/rsi/73/5?ver=pdfcov
Published by the AIP Publishing

Polarization-modulation near-field optical microscope for quantitative local dichroism mapping

L. Ramoino,[a] M. Labardi, N. Maghelli,[b] L. Pardi, and M. Allegrini
INFM and Dipartimento di Fisica, Università di Pisa, Via Buonarroti 2, I-56127 Pisa, Italy

S. Patanè
INFM and Dipartimento di Fisica della Materia e Tecnologie Fisiche Avanzate, Università di Messina, Salita Sperone 31, I-98166 Messina, Italy

(Received 15 August 2001; accepted for publication 27 February 2002)

A couple of experimental techniques have been implemented to an aperture near-field scanning optical microscopy (NSOM) to obtain reliable measurement of sample dichroism on the local scale. First, a method to test NSOM tapered fiber probes toward polarization conservation into the near optical field is reported. The probes are characterized in terms of the in-plane polarization of the near field emerging from their aperture, by using a thin dichroic layer of chromophore molecules, structured along stretched polymeric chains, to probe such polarization when approached in the near-field region of the probe. Second, to assure that the light intensity coupled in the fiber is polarization independent, an active system operating in real time has been realized. Such combination of techniques allowed quantitative imaging of local dichroism degree and average orientation by means of dual-phase lock-in demodulation of the optical signal. Translation of the coupled light polarization state in the near field has been observed for one-half of the tested probes. For the others, the tip acts as a polarizer, and therefore showed it was not suitable for polarization modulation NSOM measurements. © *2002 American Institute of Physics.*
[DOI: 10.1063/1.1470710]

I. INTRODUCTION

Among the current goals in near-field scanning optical microscopy (NSOM) are the improvements of spatial resolution as well as sensitivity to different types of optical properties. On the way to exploit new contrast mechanisms, polarization contrast techniques have been developed.[1–7] The aim of such studies has been to control the polarization properties of the near field produced by subwavelength apertures, in order to assess the dependence of the sample local optical response on polarization, and to carry out information about dichroism, magneto-optical Kerr effect, birefringence, and in general optical activity of the sample on the local scale. In general, such works have been devoted to extend to the near field some polarization-based techniques quite well known in spectroscopy and in standard optical microscopy. The biggest efforts have concerned the control of the polarization used to excite the sample.

In such direction, the main goal of the present work is to perform a direct measurement of the polarization properties of the near field produced by a real NSOM probe. Our results show indeed this as a crucial point in order to have a genuine and quantitative interpretation of measurements obtained by polarization NSOM techniques, since at present the reproducibility of NSOM apertures is under improvement.[8]

While studying polarization properties of fields produced by near-field probes, it is very important to take into account the presence of the sample, since

(i) as shown in theoretical and experimental works[9–11] the presence of the sample in the near-field region can strongly modify the throughput and emission pattern of the produced near field, and
(ii) the sample plays a fundamental role in coupling the nonpropagative near field into detectable far-field radiation.

Generally, in near-field microscopy the tip is placed at a few nanometers over the sample surface, in order to generate interaction with the near field. The far-field radiation produced by such interaction is the signal containing the information of interest, which depends on both the excitation near field and the sample optical properties. Usually, the excitation system parameters are kept constant and the detected far-field variations during a scan are considered, depending mainly on the spatial inhomogeneity of sample optical properties.

In our experiment we have used the reversed approach, acting directly on the excitation near field produced by the probe. In this respect, the means to access the actual conformation and polarization properties of the near field should be chosen in order to have a reliable description of the field properties. Usually such properties are inferred from the measured far-field pattern[11] and polarization,[3] or alternatively some photosensitive material is located within the near field and then developed to yield a fingerprint of the field distribution close to the aperture, to be read afterwards as a

[a]Present address: Institute of Physics, University of Basel, Klingelbergstr. 82, CH-4056 Basel, Switzerland.
[b]Present address: Abteilung Experimentelle Physik, University of Ulm, Albert-Einstein-Allee 11, D-89069 Ulm, Germany.

topographic feature.[12] In our approach, the *a priori* knowledge of the sample optical properties and the measurement of the far field produced by tip-sample interaction provide information about the excitation near field.[13] In particular, our goal is to characterize the polarization properties of the near field produced by a real NSOM fiber probe and to study to what extent such properties can be controlled by acting on the polarization of the light coupled into the NSOM fibers. Thus, in principle, the polarization state of the field at the NSOM tip would be known, and aimed optical scattering and spectroscopy experiments could be conducted, provided that the sample does not perturb the emitted fields too much, that is, in the cases when the passive probe approximation[14] holds.

For our measurements we have used a special dichroic sample,[15] made by diluting a high-efficiency fluorescent chromophore, a terthiophene derivative,[16] in ultrahigh molecular weight polyethylene and by subsequent casting. The PE is then mechanically stretched at suitable temperature, producing the alignment of both the polymer chains and the chromophore molecules along the strain direction. Chromophore molecules are characterized by an electric dipole momentum that is also oriented along the strain direction, leading to a dichroic optical behavior of the film. Scanning electron microscopy (SEM) microanalysis of sulphur atom performed on such samples shows that the chromophore molecules, before the stretching action, are concentrated in a thin region at the film upper surface, of about 10 μ, since they tend to phase segregate during the casting process. This means that, after the stretching (the stretch ratio of the sample used is 20), dichroic molecules are concentrated in about 500 nm thickness. Smaller values could be achieved by increasing such a stretching ratio.

The wavelength used in our experiments (488 nm) lays within the absorption region of the chromophore. The fluorescence produced by illumination with a collimated laser beam is broadband in the region from 500 to 700 nm. By changing the incident polarization, the shape of the emission spectrum is essentially unchanged. The far-field collection optics of our NSOM has been provided with a broadband interference filter (606 nm, full width at half maximum 45 nm) selecting a substantial fraction of the chromophore fluorescence emission. Detecting the intensity of emitted light provides a measurement of the absorption, which is dichroic due to the molecular orientation in the polymer matrix.

Therefore, in this setup, the sample acts as a polarization analyzer. The special property of this analyzer is that the dichroic fluorescent molecules are concentrated in a thin region close to the tip aperture. This is the region where the nonpropagative near field is concentrated and where it strongly overcomes the far-field components. This means that with our technique we can have a direct measure of the in-plane near-field polarization.

A commercial sheet polarizer is not suitable for the same purpose, since in that case, the detected signal would be composed by the intensity of the far-field light emitted by the probe at a certain polarization, plus the fraction of near-field light scattered towards the detector, at the same polarization. This gives information on the dichroism of the thin sample layer concerned by the near field along with the emitted far-field light. The use of the luminescence effect allows us to cut off the far-field component by spectral filtering.

II. EXPERIMENTAL SETUP

We have implemented our polarization modulation technique on a homemade NSOM, described in a previous publication,[17] working in emission mode and detecting light in transmission. The probes used are commercial NSOM tapered fibers (Nanonics Imaging™ FN-50) with a 50 nm nominal aperture, obtained by suitably coating the taper by a few monolayers of chromium and about 100 nm of aluminum. The tips are produced by heating-pulling technique,[18] starting from monomode optical fibers (step index type, core diameter 9 μ, monomode wavelength 1500 nm).

To act on the near-field polarization we directly turn the polarization direction of the light coupled in the NSOM fiber, as customarily done in polarization contrast NSOM.[1,4,5,6] The source is a linearly polarized Ar^+ laser at 488 nm. The laser light is circularly polarized by a $\lambda/4$ plate by setting the angle between plate axis and polarization of incident light to 45°, and then, by a turnable linear polarizer, we select the linear polarization direction to be coupled in the NSOM fiber. It is also possible to continuously rotate the polarizer, which is fixed to the rotating axis of a mechanical chopper, and to use lock-in detection to demodulate the optical signal in amplitude and phase. Therefore we obtain a measurement of dichroism degree and average orientation, respectively.

We want to focus our attention on how the real subwavelength aperture acts on the different incoming polarizations, by minimizing other effects. We assume that the knowledge of the polarization state of the light at the end of the optical fiber, where the metallized taper and the aperture are located, is not strictly relevant for what concerns the polarization produced at the aperture, since the action on polarization of the taper of a real fiber tip, and of the aperture itself, is not expected to be reproducible for different tips, even with the same nominal characteristics, due to slight differences in the geometry that are difficult to eliminate.

We have found that both our polarization turning system and the fiber coupler induce variations in the intensity of the light coupled inside the fiber depending on the polarization state of incident light. Such tests has been carried out by using a NSOM optical fiber with the tip removed, so that it was possible to measure the coupled light power. Careful alignment of the system could improve such undesired intensity modulations, but imperfections in the fiber cleavage will always induce a residual dependence of coupled power on polarization. For this reason we have implemented a special setup to exclude such effect from our system, based on an on-line monitoring of the light power coupled in the optical fiber, even in the presence of the NSOM tip. Our fibers have a transparent jacket, and upon bending some light is coupled from the core to the cladding, and, therefore, leaves the fiber, becoming detectable outside. We have found that by bending and squeezing our fibers just for few centimeters of their length, the laterally diffused light intensity is proportional to the intensity present inside the fiber, regardless of its polar-

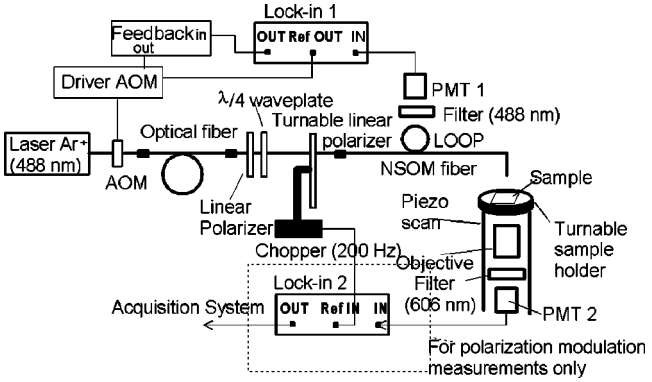

FIG. 1. Sketch of our polarization contrast NSOM setup. The signal detected by PMT1 is used as the input for the feedback system that acts on the laser beam intensity through an AOM. To increase the S/N, by means of the same AOM, the beam intensity is modulated at about 100 kHz and a lock-in amplifier demodulates the loop signal. The optical signal can be directly acquired in the case of a fixed position of the incoming polarization, while for the continuous polarization modulation technique a double-phase lock-in amplifier is needed to demodulate the signal in amplitude and phase.

ization state. To check such proportionality we have compared the diffused light intensity with the one measured at the output of our test fiber. After proper alignment of the optical system, the agreement was measured within 0.5%.

We have used the diffused signal from the bent fiber region (loop) as the input signal of a feedback circuit, acting to control the intensity of the laser light sent to the fiber in real time during the rotation of its polarization direction. This feedback circuit acts on the intensity of the laser beam before the coupling optics, through an acousto-optic modulator (AOM). The bandwidth of the feedback amplifier (about 3.3 kHz) allows us to compensate those variations of the coupled light inside the optical fiber due to the change of coupling efficiency at different polarization, as well as to the rotating polarizer mechanical instabilities, that cause small deflections of the laser beam, passing through the polarizer itself, at the same frequency ($\sim$200 Hz) at which the polarization modulation is made. In this way, the variation of the coupled light intensity recorded during a complete revolution of the linear polarizer is typically reduced from about 15% to about 2%, making it possible to characterize the effect of the tip aperture on different coupled polarizations at reasonably constant incident power level and with real-time control.

A sketch of the experimental setup is shown in Fig. 1. The light diffused by the fiber loop is detected by a photomultiplier tube (PMT1). The tip is approached normally on the dichroic sample and the light is detected in transmission using a further photomultiplier tube (PMT2) placed below the sample. The wideband interference filter is placed between the sample and such a PMT in order to select the light produced in the highly dichroic absorption-emission process. The sample is placed over a special holder that allows a complete rotation of 360° on its plane. In this way the sample acts as a turnable near-field polarization analyzer.

III. RESULTS AND DISCUSSION

First of all we have tested with far-field light the dichroic properties of our polymer sample, prepared with a stretch ratio of 20. We have measured the luminescence light intensity for different orientations between the polarization of the incident beam and the polymer strain axis. Given the intensity of incident light we can easily define T_x and T_y as the amplitude of emitted waves detected when the polarization of the excitation beam is parallel or perpendicular to the strain axis, respectively. Therefore, in general for an angle θ between polarization and strain axis, we detect an intensity

$$I(\theta) = T_y^2 + (T_x^2 - T_y^2)\cos^2\theta. \tag{1}$$

This function fits our far field data very well and gives a ratio $\gamma \equiv T_y/T_x$ of about 3, that means a factor of about 9 for the intensities. The rather low value found is mainly due to the very small thickness of the active layer, that on the other hand is essential for probing the local component of the field produced by the aperture. Therefore the chosen polymer samples act not as perfect linear analyzers; nevertheless the dichroic ratio of the analyzer can be deconvoluted from the measured emission pattern of NSOM probes by a fitting procedure.

The method employed for the characterization of the near-field polarization is the following. The NSOM fiber is approached to the polymer film surface, and the signal generated by the luminescence process of the film for different orientations of its dichroic axis, and for different directions of linear polarization of the light coupled into the NSOM fiber, is measured. In this way, for each incoming polarization, we obtain a polar diagram with the emission pattern of the produced near field. For every NSOM probe tested we have taken such data by rotating both the input polarizer and the sample by steps of 15°.

In order to avoid tip crashes while turning the sample, we have to sufficiently withdraw the probe from it. This leads to a slight change of the contact point at each approach. We have checked the homogeneity of the sample to be sufficiently high to ensure that our emission pattern measurements are not altered in a significant way by repeated approaches of the tip. We have performed a large number of NSOM scans on the polymer, finding very high homogeneity both in the sample topography and optical properties (i.e., chromophore concentration and sample transmissivity).

What is necessary for a profitable use of polarization contrast NSOM is to identify probes where the near-field polarization direction turns according to the polarization coupled into the fiber. Only such kinds of probes are suitable for polarization modulation applications.[1,4,6,19] Our method gives the chance to test with a direct measurement such property. We have found that one-half of the 10 probes tested succeeded to translate the coupled polarization beyond the aperture, while for the others we did not find such a relation. Focussing on the first-half, for a fixed incoming polarization, we typically find a polar diagram as the one shown in Fig. 2(a). The diagram results from a convolution between the sample dichroic ratio γ and the effective spatial distribution of the near field. To deconvolve the information about the latter we can define E_{paral} and E_{perp} as the components of the electric near field lying in the plane of the sample that are parallel and perpendicular to the lobe axis, respectively. For

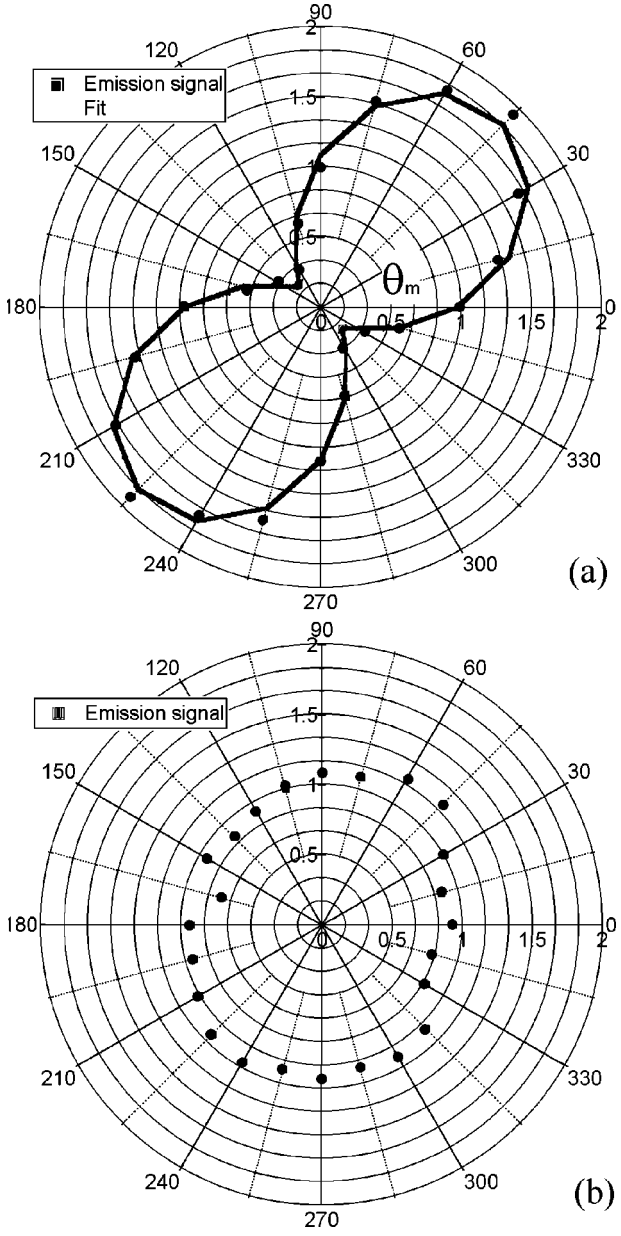

FIG. 2. Polar diagrams for two different tips. The luminescence signal is detected by turning the dichroic sample by step of 15° and is then normalized to its mean value. In case (a) the tip is able to translate the polarization to the near field and its behavior is well described by Eq. (2) giving for δ a value of 9.37 (“good tip”). In case (b) the tip is not able to translate the polarization to the near field (“bad tip”).

an angle α between this direction and the strain axis of the polymer film the detected signal will be proportional to

$$I(\alpha) \propto T_y^2 E_{\text{perp}}{}^2 [\gamma^2(\delta^2 \cos^2 \alpha + \sin^2 \alpha) + (\delta^2 \sin^2 \alpha + \cos^2 \alpha)], \quad (2)$$

where $\delta = E_{\text{paral}}/E_{\text{perp}}$. As mentioned before, this model fits well our data only for one-half of the tested probes and in such cases we carry out meaningful values for the ratio δ. For this quantity we have results typically between $\delta = 5$ and $\delta = 9$ that means a degree of polarization for the intensity of produced near field between about 25 and 80.

Fibers with a behavior well fitted by Eq. (2) for one fixed incoming polarization maintain this behavior for all the others. We can therefore use the result of the fit for every coupled polarization, to extrapolate the angle θ_m that indicates the main orientation of the near-field polarization produced by the tip aperture with respect to a fixed direction. For such fibers, it is verified that a rotation φ of the coupled light polarization leads to a corresponding variation of the lobe angle θ_m:

$$\theta_m = \theta_0 + \varphi, \quad (3)$$

where θ_0 is an offset angle depending only on the particular fiber mount. Three examples of such situations are shown in Figs. 3(a)–3(c).

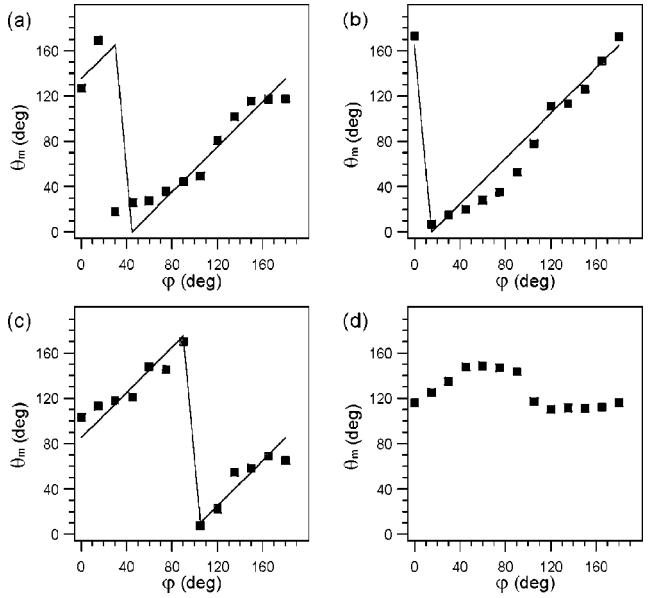

FIG. 3. Dependence of the lobe axis of the polar diagrams on the polarization direction of light coupled into the NSOM fiber. In cases (a), (b), and (c) data are well fitted by Eq. (3) (see text). Case (d) does not exhibit such a relation and the angle θ_m is roughly independent of φ. This kind of behavior affected one-half of the probes we have tested.

The behavior for the rest of the tips is quite different and it has not been possible to find any value of θ_m using Eq. (2) as a fitting function for the acquired data. An example of polar plot describing such probes is reported in Fig. 2(b). In these cases, we have chosen to define θ_m with simpler algorithms in order to determine the direction for which the intensity of the signal is the highest. In Fig. 3(d) we show an

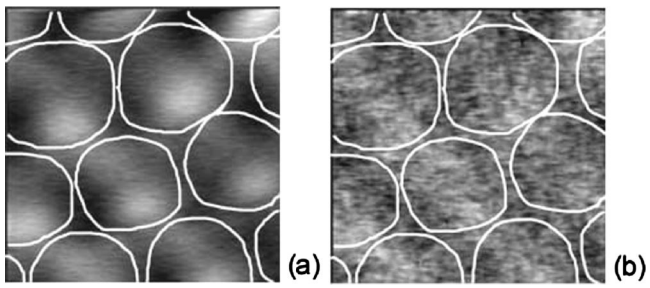

FIG. 4. Optical images (scan area $1.5 \times 1.5\ \mu\text{m}^2$) of the latex sphere test sample. The white lines reproduce the shape of the spheres obtained by the topographic image not shown. The two images have been acquired with an interval of a few minutes on the same sample area, but the results are quite different due to the different coupled polarizations.

example of the dependence of this orientation with the polarization direction of the coupled light. What we can see in Fig. 3(d), as well as in the other similar cases, is the tendency of the main direction to be almost constant. This suggests that, for such kind of probes, the aperture at the end acts as a linear polarizer.

From these data it is clear how the result of polarization contrast measurements can strongly depend on the particular tip used. To prove this point we have performed some NSOM measurements with our setup on a test sample, consisting of a monolayer of closely packed latex spheres of radius 250 nm deposited on a properly cleaned standard microscope cover glass. The material comprising the surface is chemically homogeneous, and for this reason we expect, in this case, some polarization contrast ascribable only to geometrical effects.

We have performed scans for different polarization states of the coupled light, both with a tip able to translate the polarization (''good'') and with a tip acting as a linear polarizer (''bad''). In the optical images presented in Fig. 4 we used two perpendicular linear polarizations. For the tip used in this scan we have obtained two quite different images; in particular, the signal to noise ratio (S/N) is much worse in the image of Fig. 4(b) because the probe used exhibited very different transmission coefficients for the two different coupled polarizations, that is, the tip behaved as a polarizer and, therefore, it is not suitable for polarization-modulation applications.

For comparison results obtained with a ''good'' tip are presented in Fig. 5. In Figs. 5(c) to 5(f) we show optical images acquired with four different orientations of the coupled polarization. First of all we can notice how the S/N of these four images does not drastically depend on polarization as in the previous case. Nevertheless, the four images are quite different. We can see that they present structures with shapes and position not corresponding to the topographic image represented in Fig. 5(a). This is reasonable since the near-field interacting with the sample has a defined polarization and, therefore, the center of the sphere is no longer the center of symmetry of the system. Finally, a comparison to the optical image acquired with the continuous polarization modulation, and subsequent demodulation by a lock-in amplifier [Fig. 5(b)], shows that the visible shape resembles the topographic image more closely than the images with fixed polarization in Figs. 5(c) to 5(f). In particular, the image looks more symmetric than the ones at fixed polarization. This is to be expected, since in this configuration, at least for an ''ideally good'' NSOM probe, a symmetric situation is realized and, therefore, the image should conserve the symmetry of the sample.

Our finding shows that not all the tapered fiber NSOM probes are equivalent from the viewpoint of near-field polarization properties, in spite of their nominal characteristics, can be easily explained by irregularities in the final part of the aluminum coating that break the symmetry of the aperture. In fact, it is well known[9–11] how metallic features close to the aperture can strongly modify the spatial distribution of the produced near field. For tips with more irregular structure or damages of the aperture it is reasonable to expect a much

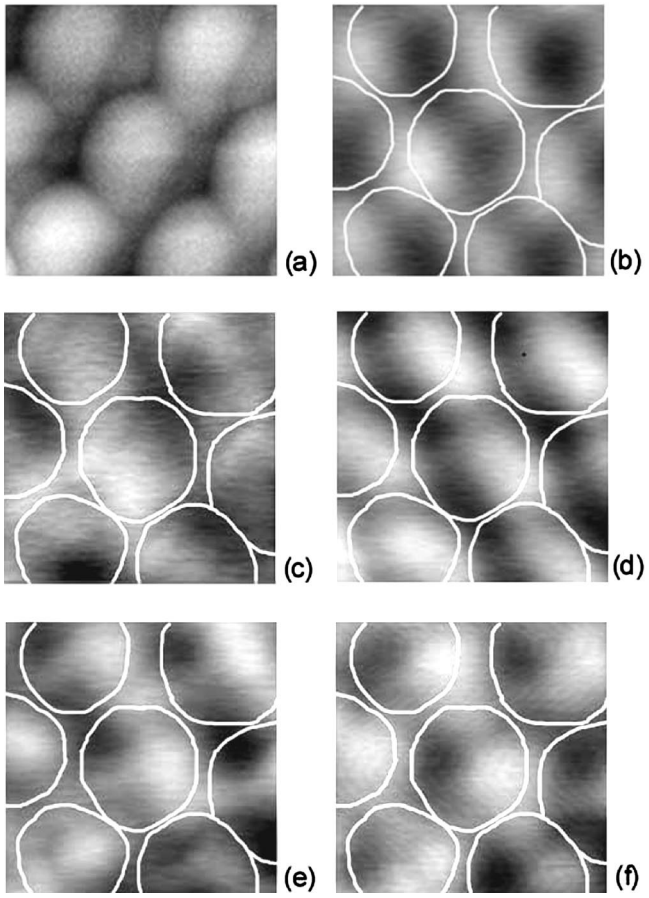

FIG. 5. Set of images (scan area $1.5\times1.5\ \mu m^2$) of the latex sphere test sample: topographic image (a), optical image obtained with polarization modulation (b), optical images for a fixed incoming polarization at 0° (c), 45° (d), 90° (e), and 135° (f).

smaller correlation between the polarization coupled inside the fiber and the near-field polarization actually available at the aperture, as well as to the polarization recorded in far field, often used to recover the one of near field.[3,11] From the point of view of the application to polarization contrast NSOM, our method looks suitable to select the probes (even from the same stock) that can be used for quantitative polarization modulation NSOM experiments.

A further application of the method described here is to near-field optical spectroscopy in those cases where the knowledge of the excitation field polarization is of importance. However, the discussed scheme is mainly valid in the case of dielectric samples, where the passive probe approximation[14] can be applied. In the case of metallic samples, for instance, the interaction is so strong that emitted light polarization properties are dramatically modified while approaching.[10,11]

Future efforts will be devoted to the analysis of the normal (z) component of the probe near-field polarization. It is indeed well known that inhomogeneous fields are characterized by the presence of longitudinal waves where the electric field can have a component parallel to the propagation vector. Theory[9] shows that for very localized fields, intensity of longitudinal (z) components becomes important and even overcomes the intensity of transverse (in plane) components analyzed in this work. However, the investigation of near-

field polarization in three dimensions requires a different typology of samples, where the chromophore orientation can be arranged also along the direction of the film thickness.

ACKNOWLEDGMENTS

We are grateful to F. Ciardelli and G. Ruggeri (Chemistry Department, University of Pisa) for providing the polymer samples, and to V. Sandoghdar and T. Kalkbrenner (Physics Department, University of Konstanz) for the latex test samples. We thank MURST for financial support through the project CIPE-Cluster 26, and EC through the TMR Network ''near-field optics for nanotechnology.''

[1] E. Betzig, J. K. Trautman, T. D. Harris, J. S. Weiner, and R. L. Kostelak, Science **251**, 1468 (1991).
[2] M. Vaez-Iravani and R. Toledo-Crow, Appl. Phys. Lett. **63**, 138 (1993).
[3] E. B. McDaniel, S. C. McClain, and J. W. P. Hsu, Appl. Opt. **37**, 84 (1998).
[4] D. A. Higgins, D. A. Vanden Bout, J. Kerimo, and P. F. Barbara, J. Phys. Chem. **100**, 13 794 (1996).
[5] T. Lacoste, T. Huser, and H. Heinzelmann, Z. Phys. B: Condens. Matter **104**, 183 (1997).
[6] T. Röder, L. Paelke, H. Held, S. Vinzelberg, and H.-S. Kitzerow, Rev. Sci. Instrum. **71**, 2759 (2000).
[7] P. Camorani, M. Labardi, and M. Allegrini, Mol. Cryst. Liq. Cryst. (in press).
[8] A. Bouhelier, J. Toquant, H. Tamaru, H.-J. Güntherodt, D. W. Pohl, and G. Schider, Appl. Phys. Lett. **79**, 683 (2001).
[9] L. Novotny, D. W. Pohl, and P. Regli, J. Opt. Soc. Am. A **11**, 1768 (1994).
[10] E. Betzig, J. K. Trautman, T. D. Harris, and R. Wolfe, Appl. Opt. **31**, 4563 (1992).
[11] C. Durkan and I. V. Shvets, J. Appl. Phys. **83**, 1837 (1998).
[12] S. Davy and M. Spajer, Appl. Phys. Lett. **69**, 3306 (1996).
[13] R. S. Decca, H. D. Drew, and K. Empson, Appl. Phys. Lett. **70**, 1932 (1997).
[14] R. Carminati and J.-J. Greffet, Opt. Commun. **116**, 316 (1995); R. Carminati, A. Madrazo, M. Nieto-Vesperinas, and J.-J. Greffet, J. Appl. Phys. **82**, 501 (1997).
[15] N. Tirelli, S. Amabile, C. Cellai, A. Pucci, L. Regoli, G. Ruggeri, and F. Ciardelli, Macromolecules **34**, 2129 (2001).
[16] Hexadecyl 2-cyano-3-[(5″-thiooctadecyl-2,2′:5′,2″-terthien)-5-yl] propenoate.
[17] P. G. Gucciardi, M. Labardi, S. Gennai, F. Lazzeri, and M. Allegrini, Rev. Sci. Instrum. **68**, 3088 (1997).
[18] B. I. Yakobson, P. J. Moyer, and M. A. Paesler, J. Appl. Phys. **73**, 7984 (1993); G. A. Valaskovic, M. Holton, and G. H. Morrison, Appl. Opt. **34**, 1215 (1995).
[19] T. Lacoste, T. Huser, R. Prioli, and H. Heinzelmann, Ultramicroscopy **71**, 333 (1998).